Steel and Composite Structures, *Vol. 21, No. 6 (2016) 1389-1410*
DOI: http://dx.doi.org/10.12989/scs.2016.21.6.1389

Hybrid of topological derivative-based level set method and isogeometric analysis for structural topology optimization

Mehdi Roodsarabi [a], Mohsen Khatibinia[*] and Seyyed R. Sarafrazi [b]

Department of Civil Engineering, University of Birjand, Birjand, Republic Islamic of Iran

(*Received January 13, 2016, Revised August 07, 2016, Accepted September 01, 2016*)

Abstract. This paper proposes a hybrid of topological derivative-based level set method (LSM) and isogeometric analysis (IGA) for structural topology optimization. In topology optimization a significant drawback of the conventional LSM is that it cannot create new holes in the design domain. In this study, the topological derivative approach is used to create new holes in appropriate places of the design domain, and alleviate the strong dependency of the optimal topology on the initial design. Furthermore, the values of the gradient vector in Hamilton-Jacobi equation in the conventional LSM are replaced with a Delta function. In the topology optimization procedure IGA based on Non-Uniform Rational B-Spline (NURBS) functions is utilized to overcome the drawbacks in the conventional finite element method (FEM) based topology optimization approaches. Several numerical examples are provided to confirm the computational efficiency and robustness of the proposed method in comparison with derivative-based LSM and FEM.

Keywords: topology optimization; level set method; topological derivative; isogeometric analysis

1. Introduction

In past decades, structural optimization as an interesting area of research has received great deal of attentions by numerous researchers. The structural optimization has ability to shorten the design cycle and to enhance the product quality (Jia *et al*. 2011). Sizing, shape and topology optimization have been considered as the classification of the structural optimization. Topology optimization can determine the optimal distribution of a given amount of material in the design domain with known loads and boundary conditions to obtain the optimal connectivity, shape and numbers of holes until the specified structural performance is maximized or minimized (Bendsøe and Sigmund 2003). For solving the topology optimization problems, a number of methods such as Optimality Criteria (OC) methods (Rozvany 1989, Rozvany and Zhou 1991), the approximation methods (Schmit and Farsi 1974, Schmit and Miura 1976, Vanderplaats and Salajegheh 1989), the Method of Moving Asymptotes (MMA) (Svanberg 1987), Evolutionary Structural Optimization (ESO) method (Xie and Steven 1993) and even more heuristic methods such as genetic algorithm (Kane and Schoenauer 1996, Fanjoy and Crossley 2000, Jakiela *et al*. 2000, Salajegheh *et al*.

∗Corresponding author, Assistant Professor, E-mail: m.khatibinia@birjand.ac.ir
[a] Graduated, E-mail: roodsarabi.mehdi.61@gmail.com
[b] Assistant Professor, E-mail: srsarafrazi@birjand.ac.ir

http://www.techno-press.org/?journal=scs&subpage=6 ISSN: 1229-9367 (Print), 1598-6233 (Online)

2009), ant colony (Kaveh *et al*. 2004) and the hybrid of metaheuristic techniques (Gholizadeh and Barati 2014, Mashayekhi *et al*. 2016) have been developed. In recent years, the level set methods (LSMs) have been proposed as an attractive alternative for topology optimization (Dijk *et al*. 2013, Luo 2013).

The LSM is known as the efficient tool of attracting, modeling and simulating the evolution of moving boundaries in many areas (Osher and Sethian 1988). The boundaries are implicitly specified by an Eulerian grid depending on the sign of the level set function. Because of modifying the implicit level set function, the boundaries of body can move, split into multiple boundaries and merge into a single boundary without any difficulty of shape parameterization and re–parameterization. The evolution of the boundary of the design domain is governed by Hamilton–Jacobi (H–J) partially differential equation and the shape velocity computed from design sensitivity analysis. For solving H–J partially differential equation, the numerical difficulties also related to the Courant–Friedrichs–Lewy (CFL) condition, periodically applied re–initializations and velocity extension schemes should be carefully utilized in the numerical process. The combination of the LSM and the shape derivative were proposed by Allaire *et al*. (2004) and Wang *et al*. (2004). The shape derivative easily handle boundary propagation with topological changes. In the conventional LSM, the final optimal design depends on the appropriate location of holes in the initial design. Incorporating the topological derivative into the LSMs was proposed by Burger *et al*. (2004) in order to measure the sensitivity of creating a small hole in the interior design domain. The topological derivative can efficiently reduce the dependency of the final optimal design on the location of holes in the initial design. Instead of the use of conventional upwind scheme for solving level set equations, the Additive Operator Splitting (AOS) method was also utilized by Lu *et al*. (1991). A survey about topological shape optimization of structures using the LSMs has been reported by Dijk *et al*. (2013) and Luo (2013).

Most of topology optimization methods utilized the conventional finite element method (FEM) for structural response analysis and sensitivity calculation. In general, the methods suffer two serious drawbacks due to a fixed FE grid used for material representation and numerical analysis. The first one is that design results are highly dependent on the initial fixed FE grid (Seo *et al*. 2010). In level set based approaches, fixed FE grid are utilized to define level set values at nodes and to analyze design models. The second drawback is that topology optimization based on FEM requires high post–processing effort in converting the optimized result to the computer–aided design (CAD) model. Using an alternative analysis method without fixed grid can overcome the first drawback. Also, unifying analysis and design models defined with CAD data have been proposed to eliminate the second drawback. In the regards, the isogeometric analysis (IGA) has been developed as a promising alternative to FEM in topology optimization (Hughes *et al*. 2005). IGA based on Non–Uniform Rational B–Splines (NURBS) basis function can be applied for both the solution field approximation and the geometry description. This leads to the ability of modeling complex geometries accurately. Studies on shape optimization and topology optimization based on IGA were presented by Wall *et al*. 2008, Cho and Ha 2009, Nagy *et al*. 2010, Qian 2010, Roodsarabi *et al*. 2016.

In this study, a hybrid of topological derivative–based LSM and IGA are proposed for structural topology optimization. Topological derivative approach is utilized to create new holes in appropriate places of the design domain, and alleviate the strong dependency of the optimal topology on the initial design. The values of the gradient vector in H–J equation of the conventional LSM are also replaced with a Delta function. In order to obtain great time advantage in the optimization procedure, a semi–implicit discretization scheme and the AOS method are

utilized to solve the level set equations. Furthermore, in the topology optimization procedure the NURBS based–IGA approach is utilized instead of in the conventional FEM. In fact, in IGA control points play the same role with nodes in FEM and B–Spline basis functions are utilized as shape functions of FEM for analysis of structure. Boundary conditions are directly imposed on control points. Numerical integration is implemented almost same with FEM in order to transform the parametric domain to master element for Gauss quadrature. In the LSM–based topology optimization procedure the design model are computed using a fixed isogeometric mesh that is unchanged during topology optimization. Hence, in this study the "Ersatz material" approach (Allaire *et al*. 2004) is adopted in order to avoid the time–consuming re–meshing process of design model topology optimization procedure. Based on the popular "Ersatz material" approach, the elements associated with the void (hole) region are modeled by a soft material. The material properties of elements intersected by the zero–level set contour are interpolated between the void and solid phase in design domain. Several numerical examples are represented to demonstrate the capability and performance of the proposed method. The numerical results of the proposed method are also compared with other LSMs and the hybrid of topological derivative–based LSM and FEM to indicate the efficiency and accuracy of the proposed method.

2. Topology optimization problem

The main aim of topology optimization is to minimize the compliance (i.e., global strain energy) over the structural domain for general loading conditions with a constraint on total material volume resources. Numerous equivalent formulations of the minimum compliance problem are proposed in the work of Allaire *et al*. (2004).

Let Ω be a bounded open set, then all admissible shapes in working domain D will be occupied by a linear isotropic elastic material with Hooke's law, Ae, in the design domain. The objective function (compliance) denoted by $J(\Omega)$ is formulated as follows

$$J(\Omega)=\int_{\Omega}\boldsymbol{f}\,\boldsymbol{u}\,dV+\int_{\Gamma_N}\boldsymbol{g}\,\boldsymbol{u}\,dS=\int_{\Omega}Ae(\boldsymbol{u})\,e(\boldsymbol{u})\,dV \tag{1}$$

where Γ_N is the Neumann (or force) boundary condition, $\boldsymbol{f}$ and $\boldsymbol{g}$ are body force and surface load, respectively; and $\boldsymbol{u}$ is the displacement field based on the following linear elasticity equations

$$\begin{cases} -div\big(Ae(\boldsymbol{u})\big)=\boldsymbol{f} & in\ \ \Omega \\ \boldsymbol{u}=0 & in\ \ \Gamma_D \\ (Ae(\boldsymbol{u}))\,n=\boldsymbol{g} & in\ \ \Gamma_N \end{cases} \tag{2}$$

where Γ_D is the Dirichlet (or displacement) boundary condition and $Ae(\boldsymbol{u})$ is the stress field.

Therefore, the standard notion for minimum compliance design problems can be mathematically defined as follows

$$\begin{aligned} &\text{Minimize}: \ J(\Omega)=\int_{\Omega}\boldsymbol{f}\,\boldsymbol{u}\,dV+\int_{\Gamma_N}\boldsymbol{g}\,\boldsymbol{u}dS=\int_{\Omega}Ae(\boldsymbol{u})\,e(\boldsymbol{u})\,dV \\ &\text{subject to}: \ \int_{\Omega}dV\le V_{max} \end{aligned} \tag{3}$$

3. Basic level set model for structural optimization

The basic LSM developed by Osher and Sethian (1988) is an efficient numerical technique for the tracking of propagating interfaces. The wide variety of successfully applications of LSM has been reported in computer vision, medical scans, seismic analysis, fluid flow, structural optimization and optimal control. It makes use of a function, ϕ, referred to as the level set function, which represents the boundary as the zero level set and nonzero in the domain. Hence, the value of the level set function is defined as

$$\begin{cases} \phi(\boldsymbol{x}(t)) > 0 : \forall \boldsymbol{x}(t) \in D \setminus \Omega \\ \phi(\boldsymbol{x}(t)) = 0 : \forall \boldsymbol{x}(t) \in \partial\Omega \\ \phi(\boldsymbol{x}(t)) < 0 : \forall \boldsymbol{x}(t) \in \Omega / \partial\Omega \end{cases} \tag{4}$$

where $D \subset R^d$ denotes the design domain, in which all admissible forms of Ω are a smooth boundary open set place in (i.e., $\Omega \subset D$), and $t \in R^+$ is time. $\partial\Omega$ is the boundary of the material domain, Ω.

The topology optimization of structures can be described by the evolution of the level set function in pseudo–time, t, with advection velocity in a normal direction, and the motion of the structural boundaries can be defined as

$$\partial\Omega(t) = \{\phi(\boldsymbol{x}(t), t) = 0\} \quad \forall \boldsymbol{x}(t) \in \partial\Omega(t) \tag{5}$$

By the total derivative of the level set function with respect to t yields, the Hamilton–Jacobi (H–J) partially differential equation as the level set equation can be obtained as

$$\frac{\partial \phi}{\partial t} + v|\nabla \phi| = 0, \quad \phi(\boldsymbol{x}, 0) = \phi_0(\boldsymbol{x}) \tag{6}$$

where v_n is the advection velocity along the normal direction of the implicit interface. In fact, the H–J equation is used to update the free structural boundaries.

Solving the H–J partially differential equation equation needs an appropriate choice of upwind difference schemes, a re–initialization algorithm and an extension velocity method, which may require excessive amounts of computational effort. Thus, this problem limits the utility of the level set methods (Osher and Fedk 2002).

4. Design sensitivity analysis and computation

4.1 Shape derivative concept

In order to solve the optimization problem (3), a based–gradient method (i.e., shape derivative) is utilized. Murat and Simon (1976) introduced a technique for constructing a shape derivative by the parameterization of domains. This approach is described as follows

$$\Omega_\theta = (\Im + \theta)\Omega \tag{7}$$

where Ω is a smooth open set domain, and $\Im$ is identity mapping in $\Re^N$, $\theta \in W^{1,\infty}(\Re^N, \Re^N)$.

The shape derivative of objective function, $J(\Omega)$: $\Re^N \to \Re^N$, is defined as the Frechet derivative in $W^{1,\infty}(\Re^N, \Re^N)$. For θ being small enough

$$J\left((\Im+\theta)\Omega\right) = J(\Omega) + J'(\Omega)\theta + O(\theta) \tag{8}$$

where $J(\Omega)$ is a continuous linear form on $W^{1,\infty}(\Re^N, \Re^N)$ given as the unique solution for the problem presented in Eq. (3).

The above equation is called Frechet derivative–based sensitivity and the sensitivity of the mean compliance (Eq. (1)) is given as follows (Garreau *et al*. 2001, Allaire *et al*. 2004)

$$J'(\Omega)\theta = \int_{\Gamma_N}\left(2\left[\frac{\partial(\boldsymbol{g}\boldsymbol{u})}{\partial n} + H\boldsymbol{g}\boldsymbol{u} + \boldsymbol{f}\boldsymbol{u}\right] - Ae(\boldsymbol{u})e(\boldsymbol{u})\right)\theta n\, dS + \int_{\Gamma_D} Ae(\boldsymbol{u})e(\boldsymbol{u})\theta n\, dS \tag{9}$$

where H is the mean curvature defined by H = div n; $\partial\Omega$ is decomposed into three parts, Γ_D, ∂D_N, Γ_O. Γ_D is an admissible Dirichlet boundary condition, such that $\Gamma_D \subset \partial D_D$; $\Gamma_N = \partial D_N \cup \Gamma_O$ is a Neumann boundary condition, where ∂D_N supports a non–homogeneous one and Γ_O supports a homogeneous one. By assuming no body force in (Eq. (1)), the objective function is also defined as

$$J(\Omega) = \int_{\partial D_N} \boldsymbol{g}\boldsymbol{u}\, dS \tag{10}$$

Therefore, the Frechet derivative of the mean compliance and the volume constraint are defined as

$$J'(\Omega)\theta = \int_{\Gamma_D}\left(-Ae(\boldsymbol{u})e(\boldsymbol{u})\right)\theta n\, dS \tag{11}$$

$$V'(\Omega)\theta = \int_{\partial\Omega}\theta(\boldsymbol{x})n(\boldsymbol{x})dS \tag{12}$$

The optimization problem is solved using the augmented Lagrangian method. Hence, based on the Lagrange multiplier, λ^k, and the penalization parameter, Λ^k, the augmented Lagrangian, $\bar{J}(\Omega)$, is defined as follows

$$\bar{J}(\Omega) = J(\Omega) + \lambda^k\left[\int_\Omega dV - V_{max}\right] + \frac{1}{2\Lambda^k}\left[\int_\Omega dV - V_{max}\right]^2 \tag{13}$$

The Lagrange multiplier and penalization parameter are updated at each iteration of the optimization process as

$$\lambda^{k+1} = \lambda^k + \frac{1}{\Lambda^k}\left[\int_\Omega dV - V_{\max}\right] \tag{14}$$

$$\Lambda^{k+1} = \alpha\,\Lambda^k \tag{15}$$

where $\alpha \in (0, 1)$ is a constant parameter. By assuming no body force, the shape derivative of the

augmented Lagrangian is obtained as

$$\overline{J}'(\Omega)\theta = \int_{\Gamma_0} v\theta n\, dS \tag{16}$$

$$v = \lambda + \frac{1}{2\Lambda}\left[\int_{\Omega} dV - V_{\max}\right]^2 - Ae(\boldsymbol{u})e(\boldsymbol{u}) \tag{17}$$

To ensure the decrease of the objective function in the level set method, the normal velocity field must be chosen appropriately. The fast descent or the steepest descent method is used, which proposed by Allaire *et al*. (2004) and Wang *et al*. (2004). The normal velocity field in the H–J equation is substituted with a normal component of this direction $\theta.n = -v$.

$$\frac{\partial \phi}{\partial t} - v\left|\nabla \phi\right| = 0.0 \tag{18}$$

4.2 Topological derivative concept

While the shape derivative is based on local perturbations of the boundary of the domain Ω, the topological derivative concept quantifies the sensitivity of the problem when the domain Ω is perturbed by the introduction of a hole. The topological derivative for all homogeneous Neumann boundary conditions on the hole is defined via

$$D_T(\boldsymbol{x}) = \lim_{|w|\to 0} \frac{J(\Omega / w_\varepsilon(\boldsymbol{x})) - J(\Omega)}{|w_\varepsilon(\boldsymbol{x})|} \tag{19}$$

where w_ε represents a small hole with radius εa, and a is constant. $|w_\varepsilon|$ is the measure of w, which is equal to $\pi\varepsilon^2 a^2$.

The topological derivative of the objective function or mean compliance on the discussion in the work of Garreau *et al*. (2001) can be obtained as follows

$$D_T J(\boldsymbol{x}) = \frac{\pi(\lambda + 2\mu)}{2\mu(\lambda + \mu)}\left\{4\mu Ae(\boldsymbol{u})e(\boldsymbol{u}) + (\lambda - \mu)tr(Ae(\boldsymbol{u}))tr(e(\boldsymbol{u}))\right\} \tag{20}$$

where λ and μ are the Lame moduli of the material. The topological sensitivity of the domain volume Ω is defined as

$$D_T V(\boldsymbol{x}) = -|w| = -\pi \tag{21}$$

where w represents a unit circle. Therefore, the topological derivative of the augmented objective function is formed the necessary ingredients as

$$\begin{aligned} D_T \overline{J}(x) &= D_T J(\Omega) + D_T\{\lambda[\int_{\Omega} dV - V_{max}] + \frac{1}{2\Lambda}[\int_{\Omega} dV - V_{max}]\} \\ &= \frac{\pi(\lambda + 2\mu)}{2\mu(\lambda + \mu)}\{4\mu Ae(\boldsymbol{u})e(\boldsymbol{u}) + (\lambda - \mu)tr(Ae(\boldsymbol{u}))tr(e(\boldsymbol{u}))\} - \lambda\pi - \frac{\pi}{\Lambda}[\int_{\Omega} dV - V_{\max}] \end{aligned} \tag{22}$$

5. Topological derivative–based LSM

A significant drawback of the conventional LSM in topology optimization is that it cannot create new holes in the design domain. Hence, the topological derivative concept can overcome this drawback. Based on the topological derivative concept, a forcing term (i.e., *wg*) is added to obtain the sensitivity of creating new holes at the interior point of the design domain of a given objective function. This term increases the level set function and later nucleates new holes in the zero level. According to the expressions in Section (3) this strategy results in a first–order H–J equation for the level set function as

$$\frac{\partial \phi}{\partial t} - v\left|\nabla \phi\right| + wg = 0 \tag{23}$$

where w is a weighting parameter which determines the influence of the topological derivative. Also, the term g is defined as follows (Huaug *et al*. 1986)

$$g = -\text{sign}\left(\phi\right) D_T \overline{J}\left(\Omega\right) \tag{24}$$

For compliance minimization, the nucleating solid areas within the void regions are pointless, because such solid regions will not take any load. Hence, holes should only be nucleated within the solid structure

$$g = \begin{cases} D_T \overline{J}\left(\Omega\right) & if \;\; \phi < 0 \\ 0 & if \;\; \phi \geq 0 \end{cases} \tag{25}$$

In order to increase stability of the LSM and obtain a good convergence, the following Delta function, instead of the measure of the gradient vector, is utilized to interpolate the scalar level set function

$$\delta_n(\boldsymbol{x}) = \frac{n}{\sqrt{\pi}} \exp(-n^2 \boldsymbol{x}^2) \tag{26}$$

where n is a positive value. Hence, the level set function is reformulated by using the Delta function as

$$\frac{\partial \phi}{\partial t} - v\,\delta_n(\phi) + wg = 0 \tag{27}$$

In this equation, the normal velocity field is substituted with the mean curvature flow and velocity to ensure a smooth design boundary or $v + \beta k$. Hence, Eq. (23) is re–constructed as

$$\frac{\partial \phi}{\partial t} - \delta_n(\phi)(v + \beta) - wg = 0.0 \;,\;\; k = \nabla\left(\frac{\nabla \phi}{\left|\nabla \phi\right|}\right) \tag{28}$$

The solving the H–J equation (i.e., Eq. (28)) based on explicit methods is time consuming procedure. Hence, in this study, the Additive Operator Splitting (AOS) scheme (Lu *et al*. 1991 and

Weickert *et al*. 1998) as a semi–implicit method is utilized for solving the H–J equation. Based on AOS scheme, Eq. (28) can be formulated as follows

$$\frac{\phi_i^{k+1}-\phi_i^k}{t}=\beta\,\delta_n(\phi^k)\left[\boldsymbol{A}_L(\phi^k)\phi^{k+1}\right]+(\delta_n(\phi^k)v-wg) \tag{29}$$

To solve Eq. (29), the level set function can be updated in the following way

$$\phi^{k+1}=\frac{1}{2}\left[U_1\ (\phi^k)+U_2\ (\phi^k)\right] \tag{30}$$

$$U_1(\phi^k)=\left[\boldsymbol{I}-2t\,\delta_n(\phi^k)\boldsymbol{A}_1(\phi^k)\right]^{-1}\left(\phi^k+t\,\delta_n(\phi^k)-t\,wg\right) \tag{31}$$

$$U_2(\phi^k)=\left[\boldsymbol{I}-2t\,\delta_n(\phi^k)\boldsymbol{A}_2(\phi^k)\right]^{-1}\left(\phi^k+t\,\delta_n(\phi^k)-t\,wg\right) \tag{32}$$

and the elements of matrix $A_L\,(\phi^k)$ is defined as follows

$$a_{ij}=\begin{cases}\dfrac{1}{h_L^2}\dfrac{2}{|\nabla\phi|_i^k+|\nabla\phi|_j^k} & ,\quad j\in\overline{N}_L(i)\\[2ex] -\dfrac{1}{h_L^2}\displaystyle\sum_{n\in\overline{N}_L(i)}\left[\dfrac{2}{|\nabla\phi|_i^k+|\nabla\phi|_n^k}\right] & ,\quad i=j\\[2ex] 0 & ,\quad else\end{cases} \tag{33}$$

where $\overline{N}_L(i)$ is the set of the two neighbors of pixel i (boundary pixels have only one neighbor) along the L directions, h is the grid size.

6. Isogeometric analysis approach

Isogeometric analysis (IGA) has developed as powerful computational approach that offers the possibility of integrating finite element analysis (FEA) into conventional NURBS–based CAD tools. The concept of the IGA is great interest in various engineering problems that is utilized for the discretization of partial differential equations. The main advantage of IGA is to utilize the NURBS basis functions that model accurately the exact geometries of solution space for numerical simulations of physical phenomena. In recent years, the IGA–based approaches have been developed and have shown many great advantages on solving many different problems such as fluid–structure interaction, shells, structural analysis and fracture mechanics (Shojaee and Valizadeh 2012, Shojaee *et al*. 2013).

6.1 B–Spline and NURBS basis function

NURBS are a generalization of piecewise polynomial B–Splines curves. The B–Spline basis functions are defined by the knot vector which is a set of non–decreasing parameters of real number (knots). A knot vector in one dimension is a non–decreasing sequence of real numbers (Hughes *et al*. 2005)

$$\Xi = \{\xi_1 \ , \ \xi_2 \ ,\ldots, \ \xi_{n+p+1}\} \tag{34}$$

where ξ_i is the i^{th} knot, i is the knot index, i + 1, 2, ..., $n + p + 1$, p is the order of the B–Spline, and n is the number of basic functions.

The half open interval $[\xi_i, \xi_{i+1})$ is called the i^{th} knot span and it can have zero length since knots may be repeated more than one, and the interval $[\xi_i, \xi_{n+p+1}]$ is called a patch. In the IGA, open knot vectors are always employed. A knot vector is said to be open if it has $p + 1$ repeating knots at the two ends. B–Spline basis functions are defined in the following recursive form as

$$N_{i,0}(\xi) = \begin{cases} 1 & \text{if} \quad \xi_i \le \xi \le \xi_{i+1} \\ 0 & \end{cases} \tag{35}$$

and

$$N_{i,p}(\xi) = \frac{\xi - \xi_i}{\xi_{i+p} - \xi_i} N_{i,p-1}(\xi) + \frac{\xi_{i+p+1} - \xi}{\xi_{i+p+1} - \xi_{i+1}} N_{i+1,p-1}(\xi) \tag{36}$$

A p^{th} degree NURBS curve is defined as follows

$$\boldsymbol{C}(\xi) = \sum_{i=1}^{n} N_{i,p}(\xi)\, \boldsymbol{P}_i \tag{37}$$

where $N_{i,p}$ (ξ) is the i^{th} B–Spline basis function of order p and P are control points, given in d–dimensional space. 1–D B–Splines basis functions built from open knot vectors are interpolatory at the ends of parametric space.

In two dimensions, B–Spline basis functions are interpolatory at the corners of the patches. The NURBS curve of order p is defined as

$$\boldsymbol{C}(\xi) = \sum_{i=1}^{n} R_{i,p}(\xi)\, \boldsymbol{P}_i \tag{38}$$

$$R_{i,p}(\xi) = \frac{N_{i,p}(\xi) w_i}{W(\xi)} = \frac{N_{i,p}(\xi) w_i}{\sum_{i=1}^{n} N_{i,p}(\xi) w_i} \tag{39}$$

where $R_{i,p}$ is the NURBS basis functions, P_i is the control point and w_i is the i^{th} weight that must be non–negative.

In the two dimensional parametric space, NURBS surfaces are constructed by tensor product

through knot vectors $\Xi = \{\xi_1, \xi_2,..., \xi_{n+p+1}\}$ and $\Psi = \{\eta_1, \eta_2,..., \eta_{m+p+1}\}$. It yields to

$$C_{i,j}(\xi,\eta) = \sum_{i=1}^{n}\sum_{j=1}^{m} R_{i,j}^{p,q}(\xi,\eta) P_{i,j} \tag{40}$$

where $P_{i,j}$ is the (i, j)th of $n \times m$ control points, also called the control mesh. The interval $[\xi_1, \xi_{n+p+1}] \times [\eta_1, \eta_{m+q+1}]$ is a patch and $[\xi_1, \xi_{n+1}) \times [\eta_1, \eta_{j+1})$ is a knot span. $R_{i,j}^{p,q}(\xi,\eta)$ is the NURBS basis function in two dimensional space

$$R_{i,j}^{p,q}(\xi,\eta) = \frac{N_{i,p}(\xi) N_{j,q}(\eta) w_{i,j}}{W_{i,j}(\xi,\eta)} \tag{41}$$

$$W_{i,j}(\xi,\eta) = \sum_{i=1}^{n}\sum_{j=1}^{m} N_{i,p}(\xi) N_{j,q}(\eta) w_{i,j} \tag{42}$$

where $N_{i,p}$ and $N_{i,q}$ are the B–Spline basis functions defined on the knot vectors over an $m \times n$ net of control points $P_{i,j}$.

The derivative of $R_{i,j}^{p,q}(\xi,\eta)$ and $W_{i,j}(\xi,\eta)$ with respect to ξ is derived by simply applying the quotient rule to Eqs. (41) and (42)

$$\frac{\partial R_{i,j}^{p,q}(\xi,\eta)}{\partial \xi} = w_{i,j} \frac{N'_{i,p}(\xi) N_{j,q}(\eta) W_{i,j}(\xi,\eta) - \dfrac{\partial W_{i,j}(\xi,\eta)}{\partial \xi} N_{i,p}(\xi) N_{j,q}(\eta)}{\left(W_{i,j}(\xi,\eta)\right)^2} \tag{43}$$

$$\frac{\partial W_{i,j}(\xi,\eta)}{\partial \xi} = \sum_{i=1}^{n}\sum_{j=1}^{m} N'_{i,p}(\xi) N_{j,q}(\eta) w_{i,j} \tag{44}$$

The domain of problem is divided into patches and each patch is divided into knot spans or elements. Patches play the role of sub–domains within which element types and material models are assumed to be uniform (Hughes *et al*. 2005). Nevertheless, many complicated domains can be represented by a single patch.

6.2 NURBS based isogeometric analysis formulation

For a 2–D linear elasticity problem with the presence of body force $\boldsymbol{f}$ and traction force $\boldsymbol{g}$, the following weak form equation is obtained by the virtual displacement method

$$\int_{\Omega} \delta\boldsymbol{\varepsilon}^T \boldsymbol{\sigma}\, d\Omega = \int_{\Omega} \delta\mathbf{u}^T \boldsymbol{f}\, d\Omega + \int_{\Gamma_t} \delta\mathbf{u}^T \boldsymbol{g}\, d\Gamma \tag{45}$$

where $\boldsymbol{\sigma}$ is the stress tensor and $\boldsymbol{\varepsilon}$ is the strain tensor. In isogeometric approach, the discretization is based on NURBS. Hence, the geometry and solution field are approximated as

$$\mathbf{x}(\xi,\eta) = \mathbf{R}\,\mathbf{P} \quad ; \quad \xi,\eta \in \Omega_{patch} \tag{46}$$

$$\mathbf{u}^h(\xi,\eta) = \mathbf{R}\,\mathbf{P} \quad ; \quad \xi,\eta \in \Omega_{patch} \tag{47}$$

where $\Omega_{patch} = \{(\xi, \eta) \mid \xi \in [\xi_1, \xi_2,..., \xi_{n+p+1}], \eta \in \eta_1, \eta_2,..., \eta_{m+q+1}\}$. The matrix–form of $R_{i,j}$ and $P_{i,j}$ can be changed into vector–form by mapping from i, j subscripts to k by

$$k = i + (j-1)n \quad ; \; with \;\; k = 1,2,\ldots,n \times m \tag{48}$$

So, the control points are defined as

$$\mathbf{P} = \{P^x_{1,1}, P^y_{1,1}, P^x_{2,1}, P^y_{2,1}, ..., P^y_{n,m}\}^T \tag{49}$$

The values of solution field at the control points, also called control variables, in the present IGA formulation are displacements and can be arranged similar to the control points in a vector form as

$$\mathbf{d} = \{d^x_{1,1}, d^y_{1,1}, d^x_{2,1}, d^y_{2,1}, \ldots, d^y_{n,m}\}^T \tag{50}$$

The matrix **R** is obtained from NURBS basis functions as follows

$$\mathbf{R} = \begin{bmatrix} R_{1,1} & 0 & R_{2,1} & 0 & ... & R_{n,m} & 0 \\ 0 & R_{1,1} & 0 & R_{2,1} & ... & 0 & R_{n,m} \end{bmatrix} \tag{51}$$

Next, the stiffness matrix for a single patch is computed as

$$\mathbf{K}_{patch} = \bar{t} \iint_{\tilde{\Omega}} \mathbf{B}^T(\xi,\eta)\,\mathbf{D}\,\mathbf{B}(\xi,\eta)\left|\mathbf{J}\right| d\xi\, d\eta \tag{52}$$

where $\bar{t}$ is the thickness, $\tilde{\Omega}$ is the parametric space, **B** (ξ, η) is the strain–displacement matrix, and **J** is the Jacobian matrix which maps the parametric space to the physical space. **D** is the elastic material property matrix for plane stress.

It is noted that in this study the standard Gauss–quadrature over each knot space is utilized for numerical integration. The proper number of Gauss points depend on the order of the NURBS basis functions.

7. Hybrid of topological derivative–based LSM and IGA

For the proposed topology optimization using the hybrid of topological derivative–based LSM and IGA, the discretization of structure is formulated in the IGA framework in this study. The objective function of the optimization problem (i.e., Eq. (1)) is also obtained based on the compliance of specify locations in structure. In IGA framework, the geometry of structure is constructed by performing knot insertion procedure on the initial geometry model shown in Fig. 1.

In this study, the initial geometry is modeled based on a bi–quadratic NURBS geometry (surface) with a number of control point. By subdividing each knot span into equal parts in ξ and η direction, the physical mesh with knot spans and the control mesh with control points are also obtained, that is shown in Fig. 2. It is noted that the position of the control points in the initial

(a) Physical mesh (b) Control mesh

Fig. 1 Initial geometry model

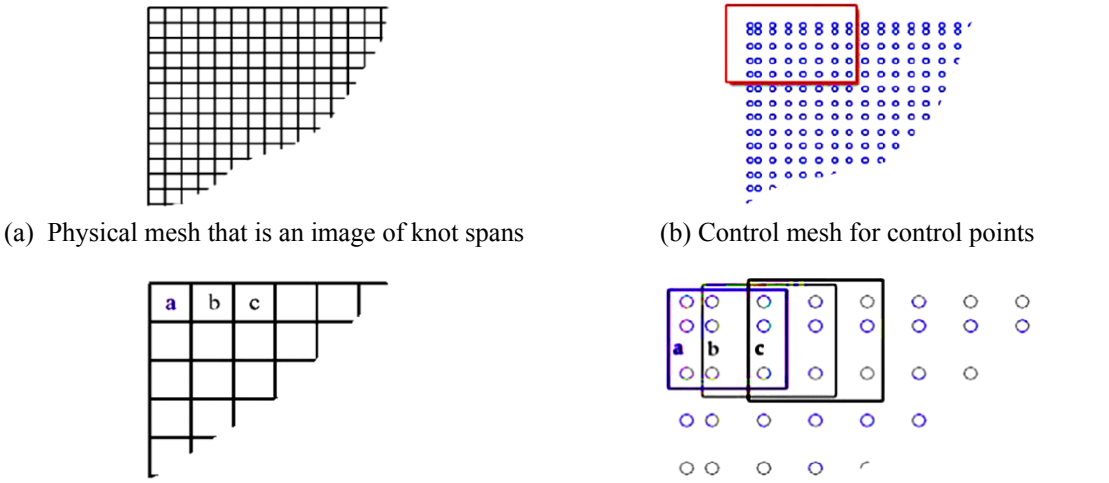

(a) Physical mesh that is an image of knot spans (b) Control mesh for control points

(c) Local view of the left top corner of physic al mesh, shows elements **a**, **b** and **c**

(d) Control points have supported on elements **a**, **b** and **c**

Fig. 2 Geometry representation for the analysis model (Shojaee *et al.* 2012)

geometry of structure has an important role in reaching the desired analysis model. Hence, the local support property of NURBS basis function is utilized. In other words, there are only $(p+1) \times (q+1)$ number of nonzero basis functions within each knot span, where p and q are the orders of NURBS. Therefore, the total number of control points per element is $(p+1) \times (q+1)$. In this study, the orders of NURBS, i.e., p and q, are equal to 2, leading to total 3×3 control points for each knot span, as shown in Fig. 2(d).

In the LSM–based topology optimization procedure IGA is implemented by using control points which play the same role with nodes in FEM and B–Spline basis functions as the shape functions of FEM for the analysis of structure. The design model are also modeled using a fixed isogeometric. For achieving this purpose, the "Ersatz material" approach (Allaire *et al*. 2004) is utilized in this study in order to avoid the time–consuming re–meshing process of design model topology optimization procedure. Based on the "Ersatz material" approach, the elements associated with the void (hole) region are modeled by a weak material. In the optimization process, the truncation strategy (Shojaee and Mohammadian 2012) is used in order to limit maximum and minimum values of normal velocities in the design domain and increase convergence efficiency and the potential of nucleation. Furthermore, filtering techniques have been proposed to avoid quick changes and suppress the non smooth variation. These schemes have been originally developed in image processing. In this study, the convolution technique proposed by Sigmund (1994) is employed in the topology optimization procedure.

8. Numerical examples

To demonstrate the efficiency and robustness of the proposed hybrid of topological derivativebased LSM and IGA, three examples of isotropic plane elasticity problem are presented in this section. Furthermore, the proposed method is compared with other LSMs the hybrid of topological derivative–based LSM and FEM. In all examples the modulus of elasticity, the Poisson's ratio and thickness are considered as 1 *Pa*, 0.3 and 0.01 *cm*, respectively. In the analysis procedure of structures, "Ersatz material" approach (Allaire *et al*. 2004) is utilized, which fills the void areas with one weak material. For this purpose, Young's modulus of ersatz material is assumed as 10^{-3} *Pa*. The order of NURBS basis functions in each direction is equal to be 2.

8.1 Cantilever beam

The design domain of a cantilever beam with a size of L = 1 cm is shown in Fig. 3. A vertical concentrated force F = 1 N is applied at the center point of the right side boundary. In the optimization procedure, the specified material volume fraction is 40%. The other parameters of LSM are also considered as Λ = 600, λ = 0, $\beta = 10^{-10}$ and α = 0.9. These parameters are selected based on the authors' experience. The time step, t, is taken as 10; and the coefficient of the topology derivative is taken as 2.

The initial geometry is modeled based on a bi–quadratic NURBS geometry with 6×4 control points. The open knot vectors are respectively {0, 0, 0, 0.125, 0.25, 0.375, 0.5, 0.625, 0.75, 0.875, 1, 1, 1} and {0, 0, 0, 0.25, 0.5, 0.75, 1, 1, 1} in ξ and η direction, thus leading to 8×4 knot spans. By subdividing each knot span into 10 equal parts in ξ and η direction, the physical mesh with

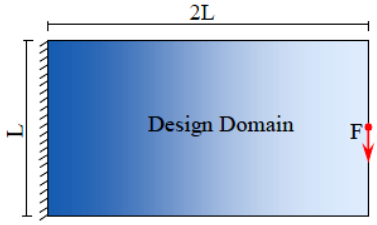

Fig. 3 A cantilever beam

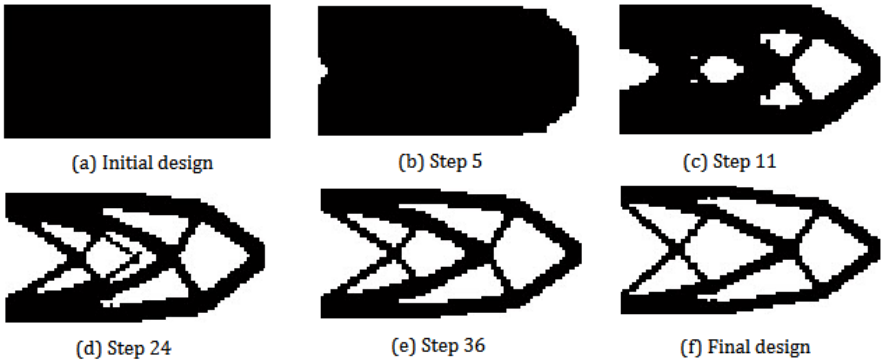

Fig. 4 The evolution process of the cantilever beam using the proposed method

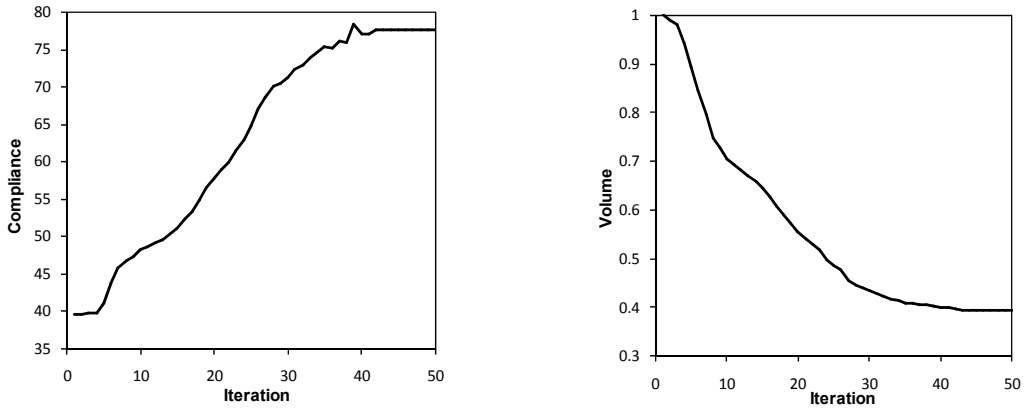

(a) (b)

Fig. 5 Convergence in the compliance and the volume ratio of the cantilever beam

80×40 knot spans and the control mesh with 82×42 control points are obtained, that is shown in Fig. 2. The evolution procedure of structural topology based on the proposed method is shown from Figs. 4(a) to (f). The final topology of the cantilever is also depicted in Fig. 4(f).

The evolutionary process of the objective function and the volume ratio are respectively displayed in Figs. 5(a) and (b). Fig. 5(a) shows the variation history of structural strain energy during optimization. Due to the volume constraint of the structure, the compliance function is increasing with the decreasing usage of material in the structure until satisfying the volume constraint, which is 40% of design domain. After that compliance is minimized, the topology of structure is constant. Fig. 5(b) shows the iteration history of material usage within the design domain during topology evolving. As can be seen from Fig. 5(b), the curve nearly leveled out at constant value at the iteration number 43.

In the next stage, FEM instead of IGA is utilized in the topological derivative–based LSM and the topology optimization of the structure is founded. To achieve this purpose, the design domain is discretized with 80×40 finite elements. In fact, the order of shape functions and the number of degree of freedoms in FEM are equal to those of IGA. The evolution procedure of structural topology based on FEM is shown from Figs. 6(a) to (b).

The final topology of the cantilever beam based on the hybrid of topological derivative–based LSM and FEM is also depicted in Fig. 6(e). It's clearly observed that the results of IGA by 3200

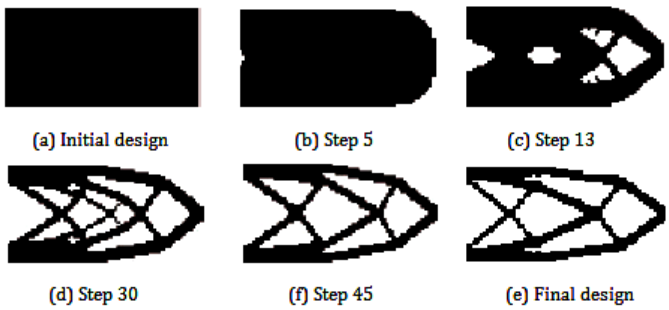

Fig. 6 The evolution process using the hybrid of topological derivative–based LSM and FEM

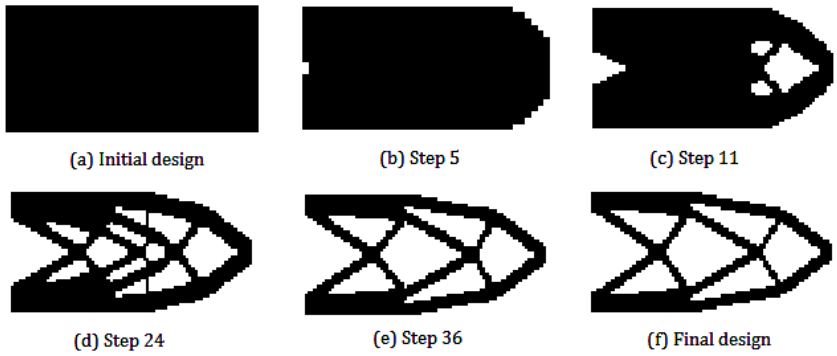

Fig. 7 The evolution process of the cantilever beam using the coarse mesh

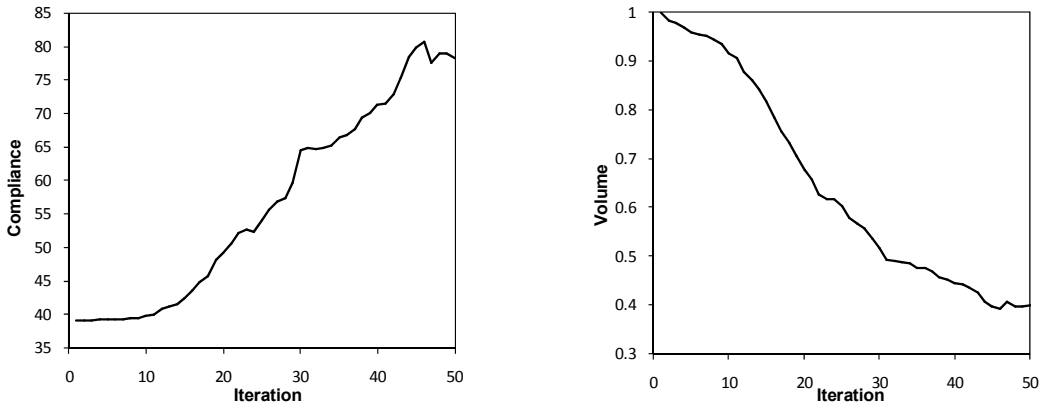

(a) (b)

Fig. 8 Convergence in the compliance and the volume ratio using the coarse mesh

elements agree well with FEA by 3200 elements. The computation time spent in the topology optimization procedure based on IGA and FEM is equal to 156.27 and 62.32 sec, respectively. The results is shown that much more computational time is spent in topology optimization based on IGA than that in FEM. One of the greatest advantages of IGA is its capability of working in exact geometry even for coarse meshes. Hence, in the following scenario a coarse mesh which contains 40×20 isogeometric mesh is selected in order to reduce the computational time of topology optimization. The evolution procedure of structural topology based on the coarse mesh is shown from Figs. 7(a) to (f). The final topology of the cantilever is also depicted in Fig. 7(f).

The evolutionary process of the objective function and the volume ratio are respectively displayed in Figs. 8(a) and (b). As can be seen from Fig. 8(b), the curve nearly leveled out at constant value at the iteration number 50.

By comparison of the final topology obtained by IGA analyzer with two mesh and FEM analyzer, the final topology is same. The other results obtained with the different schemes are also listed in Table 1.

As can be seen from Table 1, the computational time of the proposed method based on IGA with a coarse mesh is less than that through FEM scheme. Therefore, the lower iteration number

and computational time of IGA with a coarse mesh demonstrates the capability and high efficiency of the proposed method. In recent years, this example has been studied by other researchers (Shojaee and Mohamadian 2011, Shojaee *et al*. 2012, Mohammadian and Shojaee 2012, Shojaee and Mohamadian 2012). The final optimal topology obtained the proposed method of this study is compared with those obtained in other studies and shown in Fig. 9.

It can be seen from Fig. 9 that the final optimal topology obtained based on the proposed method is similar to those reported in the literature. Furthermore, the optimal results of the proposed method and other LSMs are compared and reported in Table 2.

It is obvious from Table 2 that for obtaining the optimal topology of the structure the proposed method requires less iterations than those in other LSMs. Thus, the performance of the proposed method is more efficient than other LSMs.

Table 1 Comparison of the proposed method with the hybrid of topological derivative–based LSM and FEM

Method	Iteration number of convergence	Objective function ($J(\Omega)$)	Time (sec)
LSM–IGA with 80×40 mesh	43	77.52	156.27
LSM–IGA with 40×20 mesh	50	78.28	60.62
LSM–FEM with 80×40 mesh	55	79.68	62.32

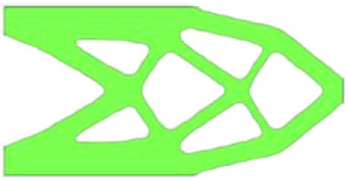

(a) The conventional LSM with FEM (Shojaee and Mohamadian 2011)

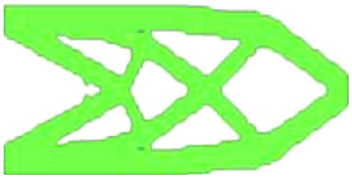

(b) The binary LSM and non-holes with FEM (Shojaee and Mohamadian 2011)

(c) The binary LSM and holes with FEM (Shojaee and Mohamadian 2012)

(d) The radial basis function LSM with IGA (Shojaee *et al*. 2012)

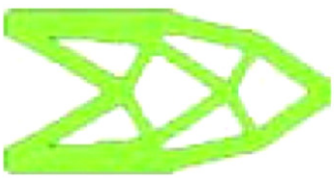

(e) The enhanced LSM with FEM (Shojaee and Mohamadian 2012)

(f) This study based on topological derivative–based LSM and IGA

Fig. 9 The comparison of the final optimal topology in this study with the other studies

Table 2 Comparison of the proposed method and other studies

Schemes	Objective function ($J(\Omega)$)	Number of convergence iterations
The conventional LSM with FEM (Shojaee and Mohamadian 2011)	63.88	200
The binary LSM and holes with FEM (Shojaee and Mohamadian 2011)	62.73	115
The binary LSM and non-holes with FEM (Shojaee and Mohamadian 2011)	64.18	100
The radial basis function LSM with IGA (Shojaee *et al*. 2012)	62.66	60
The enhanced LSM with FEM (Mohammadian and Shojaee 2012)	80.22	81
The proposed method	77.52	43

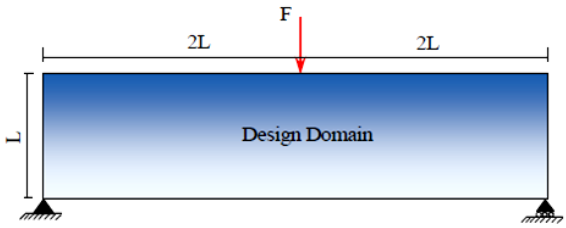

Fig. 10 Messerschmitt–Bölkow–Blom (MBB) beam

8.2 Messerschmitt–Bölkow–Blom beam

Messerschmitt–Bölkow–Blom (MBB) beam considered as the second example is the standard problem for topology optimization. The geometry model and loading conditions of MBB beam is shown in Fig. 10. The dimension of the design domain is as L = 3 cm. The downward external load

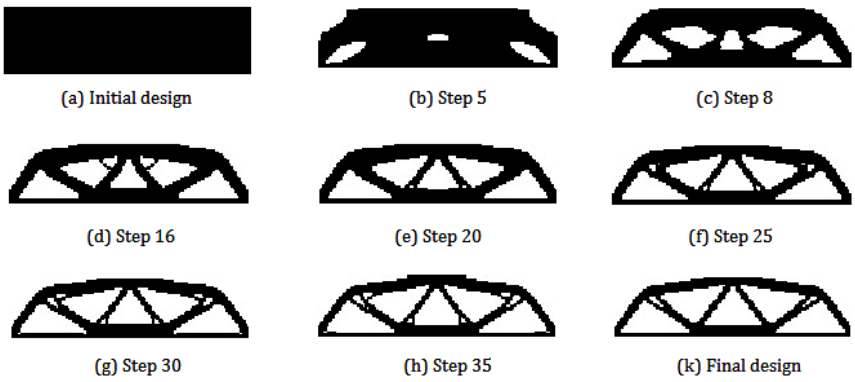

Fig. 11 The evolution process of the MBB beam using the proposed method

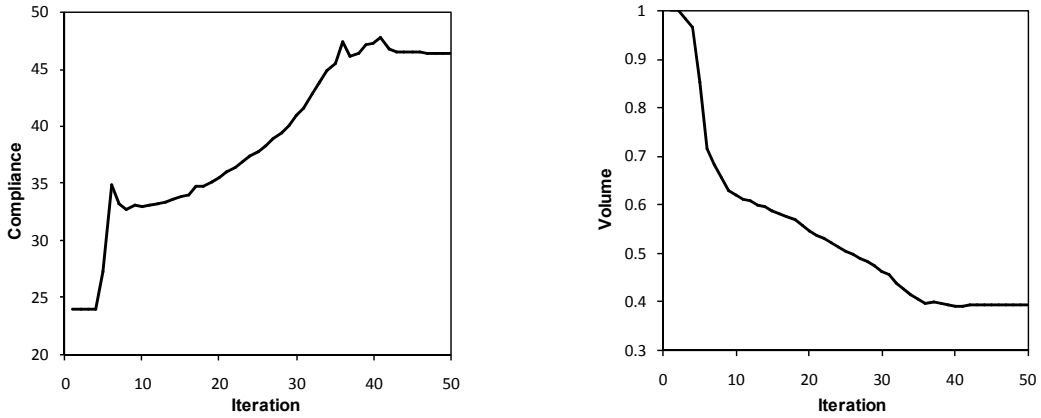

(a) (b)

Fig. 12 Convergence in the compliance and the volume ratio of the cantilever beam

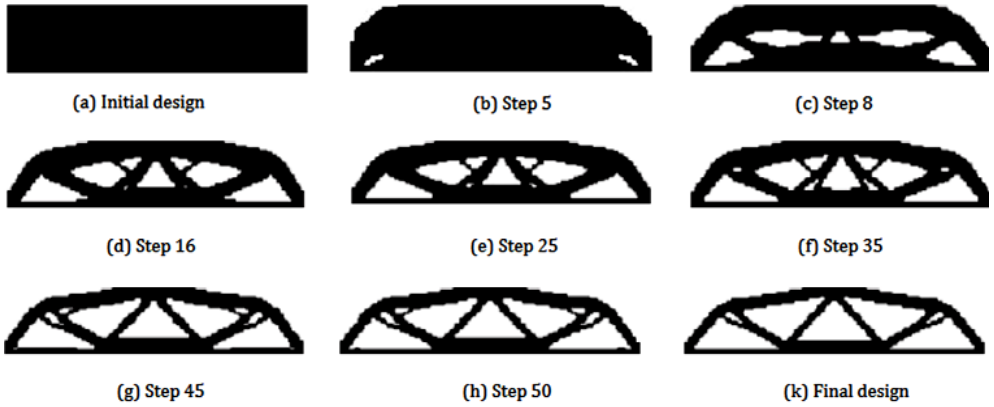

Fig. 13 The evolution process using the hybrid of topological derivative–based LSM and FEM

is located at the middle point of the upper border, and the force F = 1 N. In the optimization procedure, the specified material volume fraction is 40%. The other parameters are also considered as $\Lambda = 1000$, $\lambda = 0.001$, $\beta = 10^{-10}$ and $\alpha = 0.9$. These parameters are selected based on the authors' experience. The time step, t, is taken as 40; and the coefficient of the topology derivative is taken as 7.

The topology optimization is performed based on the proposed method with 120×30 mesh isogeometric and the topology evolving history is depicted in Fig. 11. The topology evolving history shows that the final topology is obtained in the 47 iterations.

Fig. 12(a) shows the structural strain energy variation history during optimization. Fig. 12(b) also depicts the iteration history of material usage within the design domain during topology evolving.

To show the high computational efficiency of the proposed algorithm, the problem is solved by using the hybrid of topological derivative–based LSM and FEM with 120×30 mesh. The topology evolving history is shown as in Fig. 13.

Table 3 Comparison of the proposed method with the hybrid of topological derivative–based LSM and FEM

Method	Iteration number of convergence	Objective function ($J(\Omega)$)	Time step (t)
LSM–IGA	47	46.36	9
LSM–FEM	70	46.94	9

By comparison of the final topology obtained by FEM and IGA analyzer with the same mesh, the final topology based on IGA is the same as that obtained through FEM. The other results obtained with the two different schemes are also listed in Table 3.

Based on the results of Table 3, the number iteration of the proposed method is less than that in the hybrid of topological derivative–based LSM and FEM. Therefore, this clearly indicates that the proposed method is computationally more efficient than FEM.

8.3 Michell structure

The proposed method is finally tested for the Michell structure which has been widely used as the topology optimization problem. The geometry of the Michell structure with a load, F = 1 N, applied at the center of the bottom edge is shown in Fig. 14.

The left corner of the bottom of the design domain is fixed and its right corner is simply supported. The dimension of the design domain is as L = 4 cm. In the optimization procedure, the specified material volume fraction is 40%. The other parameters are also considered as $\Lambda = 2000$, $\lambda = 0.001$, $\beta = 10^{-10}$ and $\alpha = 0.9$. These parameters are selected based on the authors' experience. The time step, t, is taken as 9; and the coefficient of the topology derivative is taken as 3.

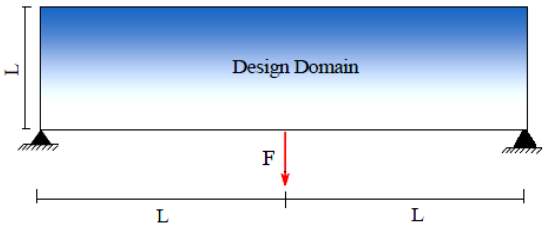

Fig. 14 Michell structure

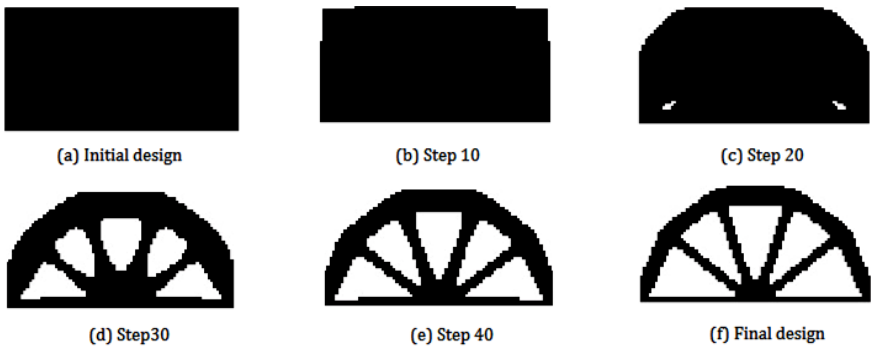

Fig. 15 The evolution process of the Michell structure using the proposed method

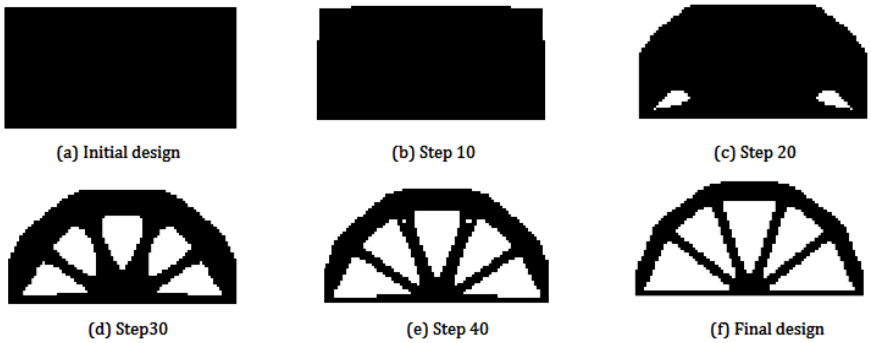

Fig. 16 The evolution process using the hybrid of topological derivative–based LSM and FEM

Table 4 Comparison of the proposed method with the hybrid of topological derivative–based LSM and FEM

Method	Iteration number of convergence	Objective function ($J(\Omega)$)	Time step (t)
LSM–IGA	66	16.3	9
LSM–FEM	70	16.3	9

The topology optimization is performed based on the proposed method with 80×40 mesh isogeometric and the topology evolving history is depicted in Fig. 15. The topology evolving history shows that the final topology is obtained in the 66 iterations.

To demonstrate the high computational efficiency and robustness of the proposed method, the problem is also optimized by using the hybrid of topological derivative–based LSM and FEM. The topology evolving history is shown as in Fig. 16.

By comparison of the final topology obtained by FEM and IGA analyzer, the final topology based on IGA is the same as that obtained through FEM. The other results obtained with the two different schemes are also listed in Table 4.

As seen from Table 4, the optimal design based on IGA is obtained in less than 66 iterations. The lower iteration number illustrates the capability and high efficiency of the propose method.

9. Conclusions

In this paper, a hybrid of topological derivative–based level set method (LSM) and isogeometric analysis (IGA) are proposed for structural topology optimization. Topological derivative approach is utilized to create new holes in appropriate places of the domain, and alleviate the strong dependency of the optimal topology on the initial design. IGA based on Non–Uniform Rational B–Spline (NURBS) functions is incorporated in the topology optimization procedure to overcome the drawbacks in the conventional finite element method (FEM) based topology optimization approaches.

The numerical examples demonstrate the merits of the proposed method in the term of the computational cost. In other words, the number iteration and computational cost of the proposed method based on the IGA analyzer with a coarse mesh is less than those in the hybrid method based on FEM analyzer. Therefore, the proposed method in comparison with other LSMs and the

hybrid of derivative–based LSM and FEM provides the computational efficiency and robustness in the structural topology optimization.

References

Allaire, G., Jouve, F. and Toader, A.M. (2004), "Structural optimization using sensitivity analysis and a level–set method", *J. Comput. Phys.*, **194**(1), 363-393.

Bendsøe, M.P. and Sigmund, O. (2003), *Topology Optimization Theory, Methods and Applications*, Springer– Verlag, New York, NY, USA.

Burger, M., Hackl, B. and Ring, W. (2004), "Incorporating topological derivatives into level set methods", *J. Comput. Phys.*, **194**(1), 344-362.

Cho, S. and Ha, S.H. (2009), "Isogeometric shape design optimization: exact geometry and enhanced sensitivity", *Struct. Multi. Optim.*, **38**(1), 53-70.

Dijk, N.P., Maute, K., Langelaar, M. and Keulen, F. (2013), "Level–set methods for structural topology optimization: A review", *Struct. Multidiscip. Opt*, **48**(3), 437-472.

Fanjoy, D. and Crossley, W. (2000), "Using a genetic algorithm to design beam cross–sectional topology for bending, torsion, and combined loading", *Proceedings of the 41st Structures, Structural Dynamics, and Materials Conference and Exhibit*, Atlanta, GA, USA, April.

Garreau, S., Guillaume, P. and Masmoudi, M. (2001), "The topological asymptotic for PDE systems: the elasticity case", *SIAM. J. Control. Optim*, **39**(6), 1756-1778.

Gholizadeh, S. and Barati, H. (2014), "Topology optimization of nonlinear single layer domes by a new metaheuristic", *Steel. Compos. Struct., Int. J.*, **16**(6), 681-701.

Haipeng, J., Beom, H.G., Wanga, Y., Lin, S. and Liu, B. (2011), "Evolutionary level set method for structural topology optimization", *Comput. Struct.*, **89**(5-6), 445-454.

Huaug, E.J., Chioi, K.K. and Kov, V. (1986), *Design Sensitivity Analysis of Structural Systems*, Academic Press, Orlando, FL, USA.

Hughes, T.J.R., Cottrell, J.A. and Bazilevs, Y. (2005), "Isogeometric analysis: CAD, finite elements, NURBS, exact geometry and mesh refinement", *Comput. Meth. Appl. Mech. Eng.*, **194**(39-41), 4135-4195.

Jakiela, M.J., Chapman. C., Duda, J., Adewuya, A. and Saitou, K. (2000), "Continuum structural topology design with genetic algorithms", *Comput. Meth. Appl. Mech. Eng*, **186**(2-4), 339-356.

Jia, H., Beom, H.G., Wang, Y., Lin, S. and Liu, B. (2011), "Evolutionary level set method for structural topology optimization", *Comput. Struct.*, **89**(5-6), 445-454.

Kane, C. and Schoenauer, M. (1996), "Topological optimum design using genetic algorithms", *Contr. Cybern.*, **25**(5), 1059-1088.

Kaveh, A., Hassani, B., Shojaee, S. and Tavakkoli, S.M. (2004), "Structural topology optimization using ant colony methodology", *Eng. Struct*, **30**(9), 2559-2565.

Lu, T., Neittaanmaki, T. and Tai, X.C. (1991), "A parallel splitting up method and its application to Navier–Stokes equations", *Appl. Math. Lett.*, **4**(2), 25-29.

Luo, Z. (2013), "A short survey: Topological shape optimization of structures using level set methods", *J. Appl. Mech. Eng.*, **2**, 123-128.

Mashayekhi, M., Salajegheh, S. and Dehghani, M. (2016), "Topology optimization of double and triple layer grid structures using a modified gravitational harmony search algorithm with efficient member grouping strategy", *Comput. Struct.*, **172**, 40-58.

Mohammadian, M. and Shojaee, S. (2012), "Binary level set method for structural topology optimization with MBO type of projection", *Int. J. Numer. Meth. Eng.*, **89**(5), 658-670.

Murat, F. and Simon, S. (1976), *Etudes de problems d' optimal design*, In: Lecture Notes in Computer Science, Springer–Verlag, Berlin, Germany, Volume 41, pp. 54-62.

Nagy, A.P., Abdalla, M.M. and Gürdal, Z. (2010), "Isogeometric sizing and shape optimization of beam structures", *Comput. Methods Appl. Mech. Eng.*, **199**(17-20), 1216-1230.

Osher, S. and Fedkiw, R.P. (2002), *Level Set Methods and Dynamic Implicit Surface*, Springer–Verlag, New York, NY, USA.
Osher, S. and Sethian, J.A. (1988), "Fronts propagating with curvature–dependent speed: algorithms based on Hamilton–Jacobi formulations", *J. Comput. Phys*, **79**(1), 12-49.
Qian, X. (2010), "Full analytical sensitivities in NURBS based isogeometric shape optimization", *Comput. Meth. Appl. Mech. Eng.*, **199**(29-32), 2059-2071.
Roodsarabi, M., Khatibinia, M. and Sarafrazi, S.R. (2016), "Isogeometric topology optimization of structures using level set method incorporating sensitivity analysis", *Int. J. Optim. Civil. Eng*, **6**(3), 405-422.
Rozvany, G.I.N. (1989), *Structural Design via Optimality Criteria*, Kluwer Academic Publishers, Dordrecht, The Netherlands.
Rozvany, G.I.N. and Zhou, M. (1991), "The COC algorithm, Part I: Cross section optimization or sizing", *Comp. Meth. Appl. Mech. Eng.*, **89**(1-3), 281-308.
Salajegheh, S., Mashayekhi, M., Khatibinia, M. and Keykha, M. (2009), "Optimum shape design of space structures by genetic algorithm", *Int. J. Space Struct.*, **24**(1), 45-57.
Schmit, L.A. and Farsi, B. (1974), "Some approximation concepts for structural synthesis", *AIAA. J.*, **12**(5), 692-699.
Schmit, L.A. and Miura, H. (1976), *Approximation Concepts for Efficient Structural Synthesis*, NASA Publisher, Washington, USA.
Seo, Y.D., Kim, H.J. and Youn, S.K. (2010), "Isogeometric topology optimization using trimmed spline surfaces", *Comput. Meth. Appl. Mech. Eng.* **199**(49-52), 3270-3296.
Shojaee, S. and Mohamadian, M. (2011), "A binary level set method for structural topology optimization", *Int. J. Optim. Civil. Eng.*, **1**(1), 73-90.
Shojaee, S. and Mohamadian, M. (2012), "Structural topology optimization using an enhanced level set method", *Sci. Iran*, **19**(5), 1157-1167.
Shojaee, S. and Valizadeh, N. (2012), "NURBS–based isogeometric analysis for thin plate problems", *Struct. Eng. Mech., Int. J.*, **41**(5), 617-632.
Shojaee, S., Mohamadian, M. and Valizadeh, N. (2012), "Composition of isogeometric analysis with level set method for structural topology optimization", *Int. J. Optim. Civil. Eng.*, **2**(1), 47-70.
Shojaee, S., Ghelichi, M. and Izadpanah, E. (2013), "Combination of isogeometric analysis and extended finite element in linear crack analysis", *Struct. Eng. Mech., Int. J.*, **48**(1), 125-150.
Sigmund, O. (1994), "Design of material structures using topology optimization", Ph.D. Thesis; Department of Solid Mechanics, Technical University of Denmark, Denmark.
Svanberg, K. (1987), "The method of moving asymptotes–a new method for structural optimization", *Int. J. Numer. Meth. Eng.*, **24**(2), 359-373.
Vanderplaats, G.N. and Salajegheh, E. (1989), "A new approximation method for stress constraints in structural synthesis", *AIAA. J.*, **27**(3), 352-358.
Wall, W.A., Frenzel, M.A. and Cyron, C. (2008), "Isogeometric structural shape optimization", *Comput. Meth. Appl. Mech. Eng.*, **197**(33-40), 2976-2988.
Wang, M.Y., Wang, X.M. and Guo, D.M. (2004), "A level set method for structural topology optimization", *Comput. Meth. Appl. Mech. Eng.*, **192**(1-2), 217-224.
Weickert, J., Romeny, B.M. and Viergever, M. (1998), "Efficient and reliable schemes for nonlinear diffusion filtering", *IEEE. Trans. Image. Process*, **7**(3), 398-410.
Xie, Y.M. and Steven, G.P. (1993), "A simple evolutionary procedure for structural optimization", *Comput. Struct.*, **49**(5), 885-896.

CC